

A NOVEL LIQUID-DESICCANT DEHUMIDIFICATION COMBINED WITH SEA SPRAY AEROSOL REMOVAL SYSTEM DRIVEN BY LOW-TEMPERATURE HEAT SOURCE

Yuze Dai, Jun Sui*, Bosheng Su, Cong Xu, Dandan Wang, Wei Han, Hongguang Jin

1 Institute of Engineering Thermophysics, Chinese Academy of Sciences, 11 Beisihuanxi Rd., Beijing 100190, PR China

2 University of Chinese Academy of Sciences, No. 19A Yuquan Rd., Beijing 100049, PR China

ABSTRACT

The air of high humidity and high sea spray aerosol (SSA) on islands or costal area always leads to the serious equipment corrosion and affects the living comfort of residents. Conventionally, the dehumidification and SSA reduction processes are separated and always consume precious electricity power and expendable materials. To simplified the procedure and reduce the energy consumption, this paper proposed a novel liquid-desiccant dehumidification system combined with sea spray aerosol removal. Based on the characteristics of liquid-desiccant dehumidification and phase transitions of the ternary solution system, the combined system can be driven by the waste heat source of 70 °C. The proposed system was simulated by the thermodynamic equilibrium model and the optimization of design parameter are presented. The results showed that the humidity ratio of the supply air can be reduced by 8.24 g/kg(dry air). The COP of this novel system is around 0.446 and its exergy efficiency can reach 12.96%. Besides, the crystallization experiment is conducted to verify the feasibility of the NaCl separation process. This study provides a new method to simultaneously remove moisture and sea spray aerosol by using low-temperature waste heat.

Keywords: Low-temperature heat utilization; Liquid desiccant dehumidification; Sea spray aerosol removal; Combination principle; System optimization

NONMENCLATURE

Abbreviations

SSA Sea Spray Aerosol

HVAC	Heating, Ventilation and Air Conditioning
<i>Symbols</i>	
a_w	water activity
COP	coefficient of performance
E	exergy
G	volume flow rate
H	enthalpy
m	mass
\dot{m}	mass per unit time
Q	heat transfer rate
t	time, h
T	temperature
y	ionic strength fraction
η_{ex}	exergy efficiency

1. INTRODUCTION

There are a large number of islands situating in the tropical marine area, with the feature of high temperature, high humidity and certain amount of sea spray aerosol (SSA). Under high-wind conditions, breaking waves and whitecaps eject large numbers of droplets into the atmosphere which are the major source of SSA. Sea spray aerosol consists of particles with radius from 0.01 μm to millimeter range, and its main component is NaCl [1]. SSA together with moisture could aggravate the electrochemical corrosion of the metal parts [2]. On the other hand, the supply air of the conventional Heating, Ventilation and Air Conditioning (HVAC) system provide poor thermal comfort under the high moisture condition [3]. Removing SSA and moisture could solve these problems.

Due to high transportation costs, power and resources on islands are more precious. Meanwhile, most waste heat from power generation unit on the islands is still not fully utilized, such as heat source below 80°C [4, 5]. So it's promising to explore new methods of removing moisture and SSA driven by waste heat with low energy level. At present, liquid-desiccant dehumidification shows the advantage on reducing the electric power consumption by utilizing low-temperature thermal energy [6, 7]. Current technologies of removing SSA requires precious electricity power and expendable materials, such as cyclone separator and high efficiency particulate air filter [8]. However, there's no reports about the single technology of dehumidification combined with SSA removal. Also, no relevant studies for SSA removal driven by thermal energy have been reported in the literature works.

In this paper, a combined liquid-desiccant dehumidification and SSA removal system driven by low-temperature heat source is proposed. By operating the proposed system, the corrosiveness of the indoor atmosphere could be reduced effectively, which is advantageous in extending service time of user equipment and saving energy and resources on the island.

2. SYSTEM DESCRIPTION

Fig 1 shows the flow chart of the proposed system. The mechanism of combination of dehumidification and SSA removal is shown as follows.

2.1 Mechanism description

A typical liquid-desiccant dehumidification process in a cross flow dehumidifier is adopted in the system [9],

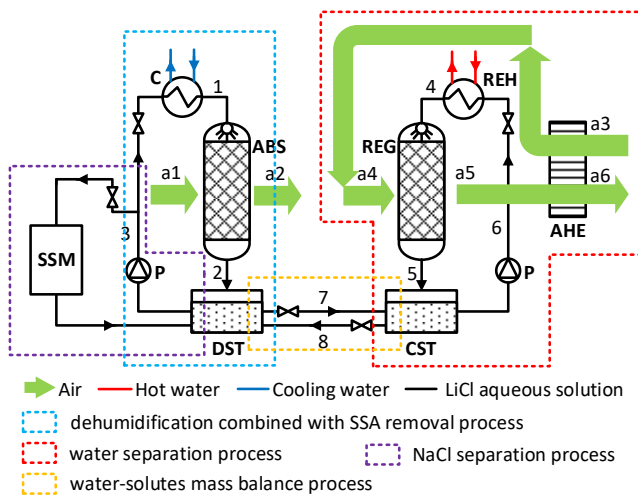


Fig 1 Flow chart of the combined liquid-desiccant dehumidification and SSA removal system driven by waste heat source

which will not be introduced in detail. Through the direct contact between the air flow and the liquid desiccant, the SSA will also be captured and absorbed by the surface of the liquid desiccant, which is similar to the process in a wet filter. With this absorption process, the moisture and SSA are removed from the fresh air together.

In order to guarantee the stability of the dehumidification performance with the dissolution of NaCl, the main component of SSA, LiCl aqueous solution is adopted as the working medium in the proposed system. With the improvement of NaCl concentration in the LiCl solution, the vapor partial pressure of the solution, which represents the dehumidification driving force, will not change rapidly for the following reason.

The vapor partial pressure of the solution is positively correlated with the water activity (a_w). Kusik and Meissner Model [10] shows a theoretical relationship between water activity of mixed solution and single-component solution, as shown in Eq. (1).

$$\ln a_w = \gamma \ln a_{w, MX}^o + (1 - \gamma) \ln a_{w, NX}^o \quad (1)$$

where γ is ionic strength fraction, $a_{w, MX}^o$ and $a_{w, NX}^o$ are the single-component water activities at the same ionic strength as the mixture. It's obvious that if the concentration of NaCl could be controlled much lower than that of LiCl, there would be little effect on the dehumidification performance of solution.

Fig 2 shows the solubility of the LiCl-NaCl-H₂O system [11]. Due to the common ion effect, the solubility of NaCl is strongly inhibited in the LiCl solution with a high concentration. For example, the maximum mass concentration of NaCl is 0.3% in the 35% LiCl solution at 25°C. Above all, a certain LiCl concentration of solution could keep a stable dehumidification performance with the absorption of SSA.

In order to ensure the stability of the system operation, it is necessary to separate the water and NaCl from the system timely. A certain amount of water in the

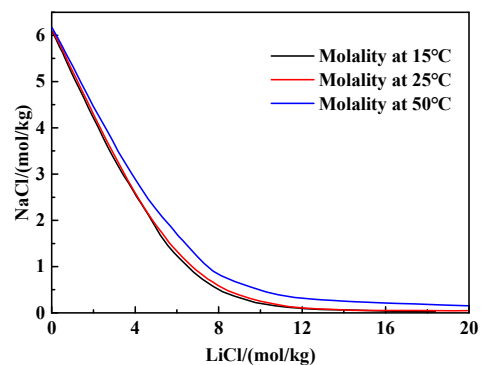


Fig 2 Solubility of the LiCl-NaCl-H₂O system

solution is volatilized and separated when the heated solution contacts air directly. The NaCl separation process is based on the phase transitions characteristics of the LiCl-NaCl-H₂O system. Previous research showed that in the eutectic point of a saturated LiCl-NaCl-H₂O system, the solid phases are NaCl and LiCl·2H₂O. Further, Table 1 gives the solutes composition of the ternary system corresponding to the eutectic point [11, 12]. When the LiCl concentration of the saturated system is lower than that corresponding to the eutectic point, the system composition moves towards the composition at the eutectic point by cooling. This makes the concentration of NaCl decreased, leading to the NaCl crystallized and separated from the system firstly. Therefore, a certain LiCl concentration of the solution could ensure the crystallization process of NaCl by cooling the saturated solution, which matches the concentration of dehumidification process. Based on the above principles, a liquid-desiccant dehumidification system combined with SSA removal is proposed and the details description is shown as followed.

2.2 process description

As shown in Fig 1, the proposed system consists of a dehumidification combined with SSA removal process, a water separation process, a NaCl separation process, and a water-solutes mass balance process. In the dehumidification with SSA removal process, the dilute solution (3) pressurized by the solution pump (P) is firstly cooled by the cooling water in a cooler (C), for improving the dehumidification capacity. Then the cooled solution (1) passes through a liquid dispenser into an absorber (ABS), and absorbs water and SSA in direct contact with the outdoor air (a1). After that, the solution (2) will flow back into the dilute solution tank (DST). In the water separation process, the pressurized concentrated solution (6) exchanges heat with the waste heat source in a regeneration heater (REH) to rise the vapor partial pressure. Then the heated solution (4) is volatilized in the

Table 1
Solutes composition of the ternary system corresponding to the eutectic point

Temperature, °C	solute composition, %	
	LiCl	NaCl
15	43.61	0.15
25	45.59	0.11
30.7	46.44	0.13
40	47.14	0.17
50	48.14	0.25
60	49.96	0.32

contact process with the air flow (a4) and flows back into the concentrated solution tank (CST), which makes the a4 temperature rises by heat transfer. Through an air heat exchanger, the sensible heat of heated air (a5) is recovered to reduce the heat loss of the system. In the NaCl separation process, part of the solution (3) flows into the sodium chloride separation module (SSM) periodically. The NaCl is crystallized and separated under a low temperature condition with a chiller. This process operates intermittently to keep the solution stationary, which promote NaCl crystal growth. In the water-solutes mass balance process, the circulation flow (7 and 8) between the CST and DST makes the water absorbed in the absorber transfer into the regenerator.

3. SYSTEM SIMULATIONS

3.1 Mathematic models

A stable thermodynamic model is established based on the energy balance theory. The thermal effect of the SSA removal process in the absorber is negligible, because the mass of the vaper absorbed is thousands of times that of SSA. The NaCl separation process is not included in the model, for the state of intermittent operation, which will be analyzed section 4.2.

Based on the mechanism description, the thermophysical properties of the ternary solution are extremely close to that of the LiCl solution, which can be calculated with the numerical equation proposed by Pátek [13]. A cross flow heat and mass transfer model reported in [14] is utilized to simulate the processes in the ABS and the REG, and the key parameter NTU_m is correlated with the corresponding experimental performance, which is set to 1.2. The design conditions of the system are shown in Table 2. All the parameters of flows could be obtained through the mass balance and energy balance of the air and solution.

In order to show the irreversible exergy destruction of the system, an exergy analysis of the proposed system is carried out, which helps to find out the improvement approaches of the system. The physical and chemical exergy are both considered, and the exergy model of solution and humid air reported in [15] is referenced.

3.2 Evaluation indices

Coefficient of performance (COP) is a common criterion to evaluate the system, which is defined as Eq. (2).

$$COP = \frac{Q_R}{Q_H} = \frac{H_{a1} - H_{a2}}{Q_H} \quad (2)$$

where Q_R is the enthalpy difference between outdoor air (a1) and supply air (a2), and Q_H is the heat input.

In order to evaluate the irreversibility of the proposed system, the exergy efficiency (η_{ex}) is adopted with the definition expressed as follows.

$$\eta_{ex} = \frac{E_{a2}}{E_H + E_{a1} + E_{a3}} \quad (3)$$

where E_H is the exergy of the heat input, and E_a is the exergy of fresh air flow.

Although the NaCl separation process will consume extra energy, the time interval of every two process can be long enough to neglect energy consumption. The minimum operating time interval is adopted to evaluate the energy consumption influence of the NaCl separation process, which is defined as Eq.(3).

$$t_{min} = \frac{m_{c,NaCl}}{\dot{m}_{a,NaCl}} \quad (3)$$

Where t_{min} is the minimum operating time interval, $m_{c,NaCl}$ is the mass of NaCl crystal separated in each NaCl separation process, and $\dot{m}_{a,NaCl}$ is the NaCl mass absorbed in the absorber per unit time.

4. RESULTS AND DISCUSSION

4.1 Case study of the proposed system

The main parameters of the system are summarized in Table 3. The system is driven by the waste heat source of 70 °C, with 39.13 kW total heat input. Partial moisture and SSA in the fresh air (3000 m³/h) is removed during the process. The reduction of humidity ratio of supply air (a2) is 8.24 g per kilogram of dry air, compared with fresh air. The same dehumidification performance can be achieved through a common condensation

Table 2
Main parameter specifications for system simulations.

Items	Value
Dry-bulb temperature, °C	30
Fresh air humidity ratio, g/kg	21.57
Air flow rate, m ³ /h	3000
Mass concentration of weak LiCl aqueous solution, %	35
Concentration difference between strong and weak solution, %	4
Cooling water temperature, °C	27
Heat source water temperature, °C	70
liquid-liquid min temperature approach, °C	5
LiCl aqueous solution flow rate, L/s	1.5
mass of solution processed in each NaCl separation process, kg	200

dehumidification process. However, during the traditional process, the air temperature corresponding to the same humidity ratio is much lower than the body temperature, which will cause the physiological discomfort. The proposed method overcomes the shortcoming and provides the specific functionality of SSA removal. Besides, the novel system can also utilize the waste heat source with a lower energy level instead of electricity power and expendable materials in the traditional SSA removal method. The specific functionality and lower energy level heat source utilization provide the proposed system with a good application prospects.

4.2 Design parameter optimization

The optimization of the internal design parameters is conducted in this part. The parameters of fresh air and supply air remain the same. The volume flow rate of solution in the absorber and crystallization temperature have a relatively significant impact on system performance, which are analyzed as follows.

Fig 3 and 4 show the effect of the volume flow rate of solution in the absorber (G_A) on system performance. With G_A decreasing from 2.4 L/s to 0.6 L/s, the solution temperature difference between the CST and DST (ΔT_{C-D}) drops from 21.53°C to 18°C, leading to less heat offset in the circulation between CST and DST. This causes the heat requirement of the water separation process decreasing, and thereby that COP of the system also rises from 0.444 to 0.452. However, the temperature of the solution stream 1 should also decrease, in order to achieve the same dehumidification performance. Under the limitation of the cooling water temperature, the

Table 3
Stream state parameters in the proposed system

State	t/°C	ξ /%	d/(g/kg(da))	m/(kg/s)
1	32	35	-	1.819
2	35.42	34.85	-	1.827
3	36.2	35	-	1.819
4	64.78	39	-	1.836
5	57.75	39.16	-	1.828
6	56.91	39	-	1.836
7	36.2	35	-	0.075
8	56.91	39	-	0.067
a1	30	-	21.57	0.957
a2	32.52	-	13.33	0.949
a3	30	-	21.57	0.957
a4	39.88	-	21.57	0.957
a5	54.88	-	29.8	0.965
a6	45	-	29.8	0.965

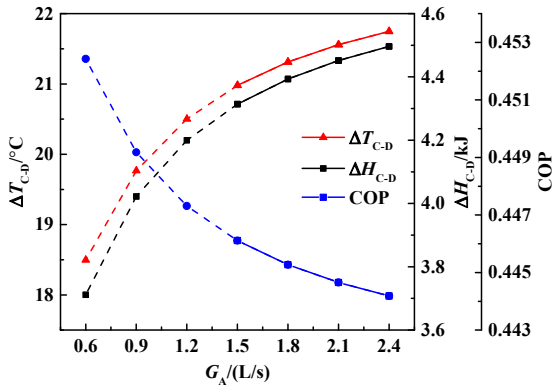


Fig 3 Effect of flow rate of solution in absorber on system performance

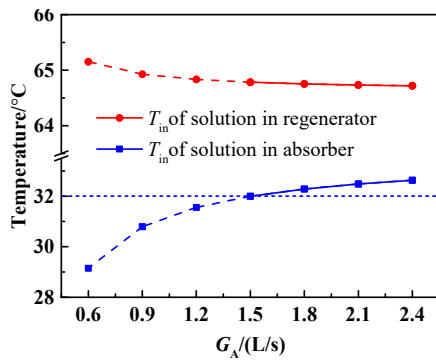


Fig 4 Effect of solution flow rate in absorber on solution temperature

lowest temperature of the solution stream 1 is 32°C, which leads to the minimum G_A of 1.5 L/s.

The NaCl separation process is considered to be periodical. The effect of crystallization temperature on the minimum operating time interval (t_{min}) is discussed under the following operating conditions. The solute of SSA in fresh air is around 5 mg/m³, and the SSA removal efficiency of the absorber is set as 70%. Fig 5 shows the mass of NaCl crystal and minimum operation cycle under different crystallization temperature. With the decrease of the crystallization temperature, the mass of NaCl crystal and t_{min} gradually improve. At a temperature of 7°C, the Mass of NaCl crystal is 0.128 kg and time interval of every two process can reach six hours. Compared with the other continuous processes in the system, the energy consumption of this process is very small and can be neglected. After the separation process, the heat input of the proposed system would also be stable by controlling the flow rate of the solution back to DST.

4.3 Exergy analysis

Table 4 is the exergy balance of the proposed system, which illustrates the exergy destruction in each component. The results shows that the exergy efficiency reaches 12.96%. The highest exergy destruction of the

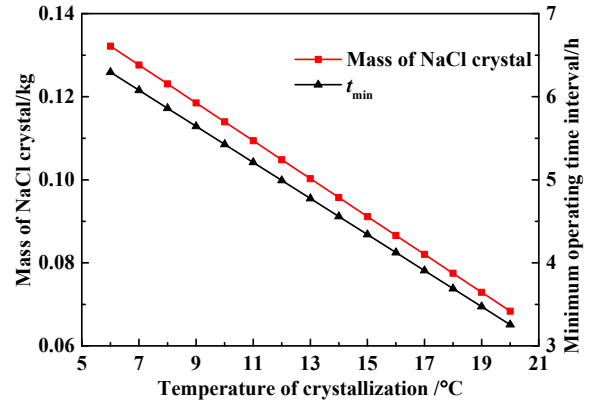


Fig 5 Effect of crystallization temperature on the NaCl separation process

proposed system occurs in the regenerator, which is 1.61 kW, i.e., 35.86% of the total exergy destruction. This is mainly because there is still a large temperature difference between the regenerated solution and the air from heat exchanger. An air preheater driven by the waste heat air is considered to be an optional plan in further exploration.

4.4 Experimental verification

To further verify the feasibility of the NaCl separation process, the key process of the system, the experiment of cooling and crystallization of LiCl-NaCl-H₂O ternary saturated solution is carried out. The mass concentration of LiCl is 30%, with an initial temperature of 30°C, and the crystallization temperature is set to be 10°C. Fig 6 shows the change of ternary saturated

Table 4 Exergy balance in the proposed system

Items	kW	%
Exergy input	4.49	100.00
Heat	4.32	96.11
Fresh air for absorption	0.09	1.95
Fresh air for regeneration	0.09	1.95
Exergy destruction and losses	3.91	87.04
1. Air handling process	0.34	7.57
Absorber (ABS)	0.34	7.57
2. Regeneration process	1.61	35.86
Regenerator (REG)	1.61	35.86
3. solution mixing process	0.41	9.08
Dilute solution tank (DST)	0.20	4.42
Concentrated solution tank (CST)	0.21	4.66
4. Heat exchange process	1.18	26.33
Cooler (C)	0.29	6.47
Regeneration heater (REH)	0.44	9.83
Air heat exchanger (AHE)	0.45	10.03
5. Other losses	0.37	8.20
Exhaust air	0.37	8.20
Exergy Output	0.58	12.96
Exergy efficiency (η_{ex}), %		12.96

solution. The results show that NaCl can be crystallized from the saturated solution through cooling process. A large number of primary crystal nuclei are formed in the solution when the degree of supersaturation reaches a certain level. Due to the mass of NaCl crystal is constant under the same crystallization temperature, the final size of the crystal particle drops with the number of the crystal nuclei rising, which means it is more difficult to separate the crystal from the solution. Parts of crystal particles in the last cycle can be retained in the crystallizer as the crystal nucleus of the next cycle, which is adopted as the optimization plan in further exploration.

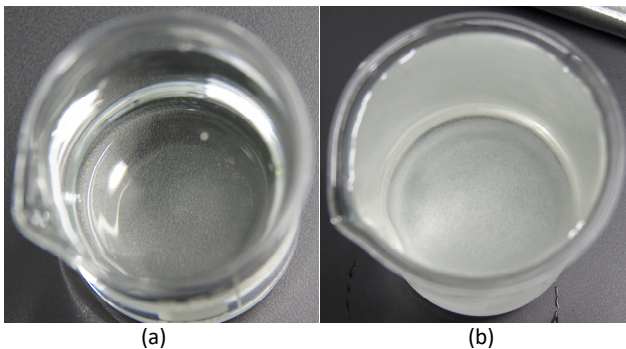


Fig 6 Change of ternary saturated solution. (a) Before cooling (b) After cooling

5. CONCLUSIONS

In this paper, a novel liquid-desiccant dehumidification combined with sea spray aerosol removal system driven by waste heat source is proposed. Based on the characteristics of liquid-desiccant dehumidification and phase transitions of the ternary solution system, the combined system can be driven by the waste heat source of 70 °C.

The proposed system was simulated by the thermodynamic equilibrium model and the optimization of design parameter are presented. The results showed that the humidity ratio of the supply air can be reduced by 8.24 g/kg(da). The COP of this novel system is around 0.446 and its exergy efficiency can reach 12.96%. The feasibility of the NaCl separation process is verified with the experiment.

The proposed method helps to reduce the corrosiveness of the indoor atmosphere effectively and has obvious advantages on extending service life time of user equipment. It makes full use of the waste heat with low energy level and shows a good performance on resources saving on islands, which has favorable prospects for application.

ACKNOWLEDGEMENT

The authors acknowledge the support of National Key Research and Development Program of China (Grant No. 2018YFB0905103) and the National Natural Science Foundation of China (Grant No. 51806213)

REFERENCE

- [1] Grythe H, Ström J, Krejci R, Quinn P, Stohl A. A review of sea spray aerosol source functions using a large global set of sea salt aerosol concentration measurements. *Atmospheric Chemistry and Physics*,14,3(2014-02-03). 2014;14:1277 – 97.
- [2] Roberge PR, Klassen RD, Haberecht PW. Atmospheric corrosivity modeling — a review. *Materials & Design*. 2002;23:321-30.
- [3] Chua KJ, Chou SK, Yang WM, Yan J. Achieving better energy-efficient air conditioning – A review of technologies and strategies. *Applied Energy*. 2013;104:87-104.
- [4] Manzela AA, Hanriot SM, Cabezas-Gómez L, Sodr e JR. Using engine exhaust gas as energy source for an absorption refrigeration system. *Applied Energy*. 2010;87:1141-8.
- [5] Zhang J, Zhou Y, Li Y, Hou G, Fang F. Generalized predictive control applied in waste heat recovery power plants. *Applied Energy*. 2013;102:320-6.
- [6] Islam MR, Alan SWL, Chua KJ. Studying the heat and mass transfer process of liquid desiccant for dehumidification and cooling. *Applied Energy*. 2018;221:334-47.
- [7] Garousi Farshi L, Mahmoudi SMS, Rosen MA. Exergoeconomic comparison of double effect and combined ejector-double effect absorption refrigeration systems. *Applied Energy*. 2013;103:700-11.
- [8] Verlaan CCJ. Performance of novel mist eliminators. Delft: Delft University of Technology; 1991.
- [9] Su B, Han W, Jin H. An innovative solar-powered absorption refrigeration system combined with liquid desiccant dehumidification for cooling and water. *Energy Conversion and Management*. 2017;153:515-25.
- [10] Kusik CL, Meissner, H.P. Electrolyte activity coefficients in inorganic processing. *American Institute of Chemical Engineers*. 1978;74:14-20.
- [11] Lovera JA, Graber TA, Galleguillos HR. Correlation of solubilities for the NaCl+LiCl+H₂O system with the Pitzer model at 15, 25, 50, and 100°C. *Calphad*. 2009;33:388-92.
- [12] Farelo F, Fernandes C, Avelino A. Solubilities for Six Ternary Systems: NaCl + NH₄Cl + H₂O, KCl + NH₄Cl + H₂O, NaCl + LiCl + H₂O, KCl + LiCl + H₂O, NaCl + AlCl₃ + H₂O, and KCl + AlCl₃ + H₂O at T = (298 to 333) K. *Journal of Chemical & Engineering Data*. 2005;50:1470-7.
- [13] Pátek J, Klomfar J. Thermodynamic properties of the LiCl–H₂O system at vapor–liquid equilibrium from 273K to 400K. *International Journal of Refrigeration*. 2008;31:287-303.
- [14] Liu X, Jiang Y, Qu K. Heat and mass transfer model of cross flow liquid desiccant air dehumidifier/regenerator. *Energy Conversion and Management*. 2007;48:546-54.
- [15] Su B, Han W, Sui J, Jin H. Feasibility of a two-stage liquid desiccant dehumidification system driven by low-temperature heat and power. *Applied Thermal Engineering*. 2018;128:795-804.